HHS Public Access

Author manuscript

J Phys Chem B. Author manuscript; available in PMC 2016 October 17.

Published in final edited form as:

J Phys Chem B. 2016 September 8; 120(35): 9387–9394. doi:10.1021/acs.jpcb.6b07212.

2D IR Study of Vibrational Coupling Between Azide and Nitrile Reporters in a RNA Nucleoside

Andrew J. Schmitz[a], **David G. Hogle**[a], **Xin Sonia Gai**[b], **Edward E. Fenlon**[b], **Scott H. Brewer**[b], and **Matthew J. Tucker**[a,*]

[a]Department of Chemistry, University of Nevada, Reno, NV 89557, USA

[b]Department of Chemistry, Franklin & Marshall College, Lancaster, PA 17604-3003, USA

Abstract

The vibrations in the azide, N_3, asymmetric stretching region and nitrile, CN, symmetric stretching region of 2'-azido-5-cyano-2'-deoxyuridine (N_3CNdU) are examined by two-dimensional infrared spectroscopy (2D IR). At earlier waiting times, the 2D IR spectrum shows the presence of both vibrational transitions along the diagonal and off-diagonal cross peaks indicating vibrational coupling. The coupling strength was determined from the off-diagonal anharmoncity to be 66 cm^{-1} for the molecular distance of ~7.9 Å based on a structural map generated for this model system. In addition, the frequency-frequency correlation decay is detected, monitoring the solvent dynamics around each individual probe position. Overall, these vibrational reporters can be utilized in tandem to simultaneously track global structural information and fast structural fluctuations.

Graphical Abstract

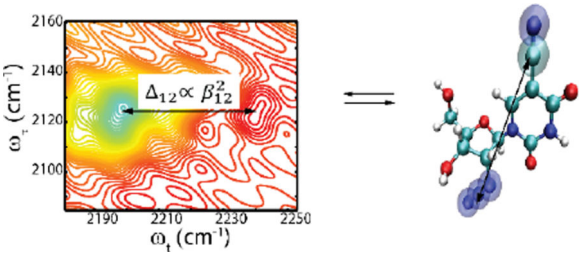

Introduction

Infrared reporters, such as nitriles and azides, have become widely utilized as vibrational probes to study biomolecules due to their sensitivity to local environment, small size, overall chemical stability, and relatively localized transitions.[1–10] In particular, ultrafast measurements of the stretching mode of the nitrile group in a variety of biological systems have provided insight into site-specific vibrational dynamics.[11–17] Since both the N_3 and CN

*Corresponding Author. Phone: (775)-784-4376 Fax: (775)-784-6804. mtucker@unr.edu.

Supporting Information. Further details on Gaussian calculations, coupling strength decay data and TDC is available. This material is available free of charge via the Internet at http://pubs.acs.org.

transitions are found in a spectrally transparent region of most biological molecules, several studies have benefited from the isolated and relatively sharp spectral feature to investigate beta-amyloid aggregation, drug-enzyme interactions, and other biological processes.[1, 2, 5, 11, 18, 19] Despite a wide variety of applications, the relatively small absorption cross section of the nitrile vibrational transition limits its feasibility for use in nonlinear IR spectroscopy due to the need of much higher concentrations than desirable for biological systems. However, several alternatives have recently been developed so that more suitable vibrational reporters can be chosen for a desired application within a biological system.[20–24]

One example where the azide group has shown much promise is seen in the study of the nucleoside, 2'-azido-2'-deoxyuridine.[12] The absorption cross section of the N_3 transition is one order of magnitude greater than nitriles allowing lower concentrations to be utilized. Specifically, the aliphatic azide substitutions are stable under most conditions and often avoid accidental Fermi resonances, allowing the azide reporter to more effectively detect local environment in peptides, proteins, and nucleosides.[2, 12, 25–27] Both the N_3 transition and the CN transition have many similar spectral properties and a direct comparison of these probes has been documented using 2'-azido-5-cyano-2'-deoxyuridine (N_3CNdU).[10] The changes in vibrational frequency resulting from hydrogen bonding and sensitivity to local electric field changes of both localized infrared transitions offer many advantages to studies of structural dynamics.[21, 24] Further studies have extended the application of these probes in nucleosides to infrared, 2D IR, and NMR experiments.[28, 29] The sensitivity of these reporters to the local environment[1, 2, 8, 28] and hydrogen bonding[2, 5] provides an avenue to track these dynamics by 2D IR methods using chemical exchange[30, 31] and spectral diffusion.[11–13, 17]

Two-dimensional infrared photon echo (2D IR) spectroscopy has shown utility in both observing and understanding vibrational properties including spectral diffusion, inter-mode coupling, conformational analysis, chemical exchange, and many others.[6, 30, 32–36] Furthermore, 2D IR can provide structural information[37] via vibrational coupling in a similar way to many traditional spectroscopic rulers,[38, 39] such as EPR and FRET. While energy transfer has been observed for azide and nitrile anions in solution by 2D IR[40, 41] and coupling has been suggested in the linear IR for two isotopomeric CN probes,[42] there is no such 2D IR study on the direct vibrational coupling between these two different reporters within a single biological system. Here, we report the 2D IR of the N_3 and CN region of N_3CNdU and capture the direct vibrational coupling between these probes in water. In addition to demonstrating the utility of this 'spectroscopic ruler' for biomolecules, we show the capability to detect site-specific dynamics at two positions simultaneously. While this study focuses on a small-molecule model system, the observed coupling suggests two reporters can be utilized as a structural tool to gain distance and dynamic information in larger biomolecular systems.

Although difficulties have been encountered for incorporating azide reporters into nucleic acids using standard methods,[43–45] several approaches for the incorporation of stable azide and nitrile groups into DNA and RNA has been successful recently.[3, 28, 29, 42, 46] With these synthetic approaches, N_3 and CN probes can be placed virtually anywhere providing a useful

monitor of site-specific dynamics in environments such as the major groove, minor groove, and phosphate-sugar region. Herein, we demonstrate the effectiveness of a pair of vibrational reporters as tools to investigate structural and dynamic aspects of different regions of DNA and RNA aptamers using 2D IR.

Materials and Methods

Sample Preparation

The synthesis of N_3CNdU is described in our previous publication.[10] In short, dimethoxytrityl-protected 2'-amino-2'-deoxyuridine was converted to the 2'-azide through a copper-catalyzed diazotransfer reaction with triflic azide. Bomination of the uracil followed by cyanation with potassium cyanide and detriylation with dichloroacetic acid afforded N_3CNdU in a yield of 12.5% for the four steps.

Linear and 2D IR Method

A solution of 15–20 mM N_3CNdU in H_2O was used for both 2D IR and FTIR experiments. The sample was placed in a Harrick sample cell with CaF_2 windows and a path length of 56 μm. The linear IR spectrum was measured using a Nicolet 6700 FTIR spectrometer.

Fourier-transform limited 80-fs pulses with a central wavelength of 4580 nm were used in the 2D IR experiments. Each of the three laser pulses have an energy, ~ 1 μJ, with wave vectors k_1, k_2, and k_3, incident to the sample to generate a signal in the direction $k_s = -k_1+k_2+k_3$ with the ordering 123 (rephasing) and 213 (nonrephasing). To obtain absorptive spectra, the rephasing and nonrephasing 2D frequency spectra were properly phased and combined. To observe any changes in the spectral characteristics, the waiting time, T, between the second and third pulse, was varied from 0 to 3 ps. After appropriate Fourier transforms along the coherence, τ, and detection, t, axes, the 2D IR spectra were plotted as ω_τ vs. ω_t.[47] The vibrational relaxation times, T_{10}, for the two main transitions were estimated from the decay of signal strength of the $\nu=0 \rightarrow \nu=1$ transition in the 2D IR spectrum at different waiting times and fitted to a single exponential function, $A=A_0 e^{-\frac{T}{T_{10}}}$.

Computations

Gaussian09 *Ab Initio* Density Functional Theory (DFT) calculations of N_3CNdU were performed using B3LYP/6-31+G** level of theory with implicit solvation model of water calculated by a self-consistent reaction field (SCRF). The solvation model considered was the conducting polarizable continuum model (CPCM). For all N_3CNdU structures, an optimization was first performed using B3LYP/6-31+G** in the given solvent model, thereby obtaining frequency and energy data. These optimizations were used to determine the coupling constant using the finite difference method (FDM) as explained by Torii and Tasumi.[48] To implement this approach, the molecule was displaced along the normal modes of the nitrile and azide functional groups of N_3CNdU by a small amount (0.03 Å) and a single point energy calculation was performed. These energies were used to calculate the vibrational coupling through the second derivative of the energy with respect to the normal modes discussed below. The dihedral angle along the C-N bond between the base and sugar rings of the nucleoside, defined by atoms shown in Figure S1 in SI, was rotated from −180°

to 180° to map out the potential energy surface along this degree of freedom. These different structures were optimized with the dihedral angle held fixed and the rest of the molecule allowed to relax to an optimal configuration. The energy, angle between the nitrile and azide dipoles, and coupling constants were then calculated for each structure.[49, 50] In this way, a structural map of the distance between the two reporters was generated corresponding to specific angles between the transition dipoles and the calculated coupling constants for comparison to experiment.

Results

Linear and 2D IR Spectroscopy

The linear IR spectrum of N_3CNdU in water exhibits two bands in the region between 2050–2300 cm^{-1} (Figure 1a). The two transitions are observed at 2124 and 2242 cm^{-1}, which correspond to the asymmetric stretching mode of the N_3 and the symmetric stretching mode of CN, respectively. The FWHM was measured to be 26 cm^{-1} for the N_3 and 10 cm^{-1} for the CN mode. The observed separation between the two transitions in the infrared spectrum is approximately 118 cm^{-1} with the peak extinction ratio between the N_3 to CN transitions of approximately 2.7.

The 2D IR spectra of N_3CNdU in water has two positive peaks along the diagonal at positions $\omega_\tau = \omega_t = 2124$ cm^{-1} and $\omega_\tau = \omega_t = 2242$ cm^{-1} corresponding to the ν=0 → ν=1 transition of the N_3 asymmetric and the CN symmetric modes, respectively (Figure 1c). The negative peak, resulting from the ν=1 → ν=2 transition, of the azide mode is shifted along the ω_t axis to $\omega_t = 2085$ cm^{-1} indicating an anharmonicity ca 39 ± 1.0 cm^{-1}. Similarly, a shifted negative peak for the nitrile mode appears at $\omega_t = 2216$ cm^{-1} which indicates the diagonal anharmonicity is 0.67 times less than that of the azide mode. In the region of the CN transition, a small positive peak is observed below the main transition likely due to a Fermi resonance, which have been often identified for other azide and nitrile reporters in different molecules.[1, 6, 51] Since the peak extinction of the N_3 transition is roughly 2.7 times larger than the CN transition in the FTIR spectrum, it is expected that the azide signal would approximately 7 times larger in the 2D IR spectrum. Thus, the spectrum is dominated by the peaks arising from the N_3 transition. As a result of the population relaxation (T_{10}), the positive diagonal signals decay during the waiting time, T, with a time constant of 1.1 ± 0.1 ps and 2.8 ± 0.3 ps for azide and nitrile, respectively (Figure 2). At later times, the intensity of N_3 transition becomes similar to CN signal due to the nitrile group's significantly longer vibrational lifetime.

Noticeable cross peaks are also observed between the azide and nitrile transition in the off-diagonal region of the 2D IR spectra (Figure 1d and 2a–c). The positive peak is located at $\{\omega_\tau,\omega_t\} = \{2122,2242\}$ cm^{-1}. The negative peak is red shifted to $\omega_t = 2198$ cm^{-1} corresponding to the off-diagonal anharmonicity of 44.0 ± 3.3 cm^{-1}. The intensities of the off-diagonal peaks are maximal at the earliest time (T=0) and decay exponentially as a function of the waiting time, T (SI Figure S2). By 1 ps, the cross peak intensity has decayed by more than 25% and these 2D IR transitions become significantly less pronounced in the spectrum (Figure 2).

Both diagonal peaks are tilted and elongated along the diagonal at the earliest waiting times as a result of significant inhomogeneous broadening (Figure 3). As the waiting time increases, the shape of the peaks become more circular, giving evidence of the loss of frequency correlation (spectral diffusion) due to the fluctuations in the vibrational frequency, as shown in prior publications.[12, 52] This significant spectral diffusion is clearly observed through the slope at the intersection of the positive and negative peaks[53] of both the azide and nitrile group. It should be noted that the CN transition (ν=0 → ν=1) is somewhat distorted at later times due to the weaker dipole strength of the nitrile and the influence of scatter leading to a lower signal-to-noise ratio.

The loss of correlation can also be observed by the center line slope (CLS) method. With this method, a line along the longitudinal axis of the ellipse passing through the zeroth contour is used to measure the change in the slope of the diagonal peak. This is achieved by determining the maximum intensity of ω_t along several horizontal slices of ω_τ for the peak corresponding to the ν=0 → ν=1 transition. At T=0, the line is parallel with the diagonal line of the contour plot and it becomes more vertical at later waiting times, T, indicating complete loss of correlation. The correlation decay is plotted with inverse of the CLS, $[S(t)]^{-1}$, over waiting time and fitted to a single exponential decay function $A=A_0e^{-\frac{T}{\tau}}$, where τ is the decay constant.[54, 55] Through the CLS analysis, the correlation decay time constants from the spectral diffusion in water were measured for both modes (Figure 4). These frequency-frequency correlation decays[53–55] illustrate that each individual reporter is capable of detecting the local vibrational dynamics and timescales associated them. The correlation decay times for azide and nitrile were determined to be 1.4 ± 0.1 ps and 1.3 ± 0.2 ps, respectively. Both vibrational reporters exhibit a similar decay time suggesting each transition is exposed to similar dephasing mechanisms. Since both correlation decays do not start from unity, it is also expected that a significant portion of the spectral diffusion comes from homogeneous components.

Computational Results

To confirm the identity of the transitions and determine the transition dipole strengths, Gaussian09 DFT frequency calculations were computed after optimization. As expected, the azide and nitrile normal modes were the only two transitions observed in the spectral region corresponding to the N_3 asymmetric mode and the CN symmetric mode. The transition dipole strengths were calculated to be 0.474 Debye for N_3 and 0.198 Debye for CN vibrational modes with an angle of 60 degrees between the transition dipoles. Transition densities were determined by calculating the difference in the electron density from the equilibrium structure after a displacement of ±0.03 Å along each normal mode (Figure 5a and b). From these plots of transition densities with gradient of 0.002 esu/bohr, it is clear that the modes are localized with respect to the N_3 and CN atoms.

The geometry-optimized structure, shown in Figure 1b, has a dihedral angle (defined in Figure 5c) of 10.21°. In order to generate a structural map of the distance as a function of the angle between the dipoles and the vibrational coupling, the conformation of the molecule was varied by rotation around a dihedral angle (shown in Figure 5c) and the energy relative to the minimized structure was computed upon minimization (Figure 5d). Three energetic

minima arise along the potential energy surface (PES) located at 1, 2, and 3, with the original geometry optimized structure exists in minimum 2. Minima 2 and 3 exist within the thermal equilibrium while 1 is significantly higher in energy along this PES. The energies of the different conformations further suggest that the minimum at position 3 is the most thermodynamically favored. However, upon further computations testing different solvation models, it was determined that the conformation space of the PES around position 3 shows only a very shallow local minimum that is not thermodynamically favored, see SI.

At each dihedral angle the coupling constants between the modes were calculated using finite difference method. The angle between the dipoles was also computed for each point along the surface. In minima 1, 2 and 3 of the PES, the average value of the coupling constant was determined to be 47.6 cm^{-1}, 62.0 cm^{-1}, and 35.7 cm^{-1}, respectively. The corresponding average angle between the dipoles for minima 1, 2, and 3 were measured as 83.7° ± 10.2°, 64.3° ± 8.9°, and 77.72° ± 7.8°, respectively. Although only the relevant values are reported at these important regions of the PES, the coupling constants and the angles between the dipoles were calculated for each dihedral angle. It should be noted that a large variance was observed in the values of the coupling constants and corresponding angles along the PES. The distance between the dipoles was also measured for each dihedral angle and the range varied from 5.0–8.5 Å.

Discussion

The FTIR spectrum of 2’-azido-5-cyano-2’-deoxyuridine in water has two transitions in the region of 2050–2300 cm^{-1} arising from the asymmetric stretch of N_3 and the symmetric stretch of CN. The overall shape of both vibrational transitions can be fit to a single Gaussian profile.[7, 12] The presence of these two reporters within a close proximity in the same molecule results in significant vibrational coupling between their dipoles. As a result, the relative intensities of the infrared transitions are sufficiently different than expected from prior literature[7, 12, 28] as well as the calculated transition dipole ratio. The observed vibrational frequencies and relative intensities of the linear IR spectrum can often be predicted from the solutions to the Hamiltonian shown below:

$$H = \begin{pmatrix} \varepsilon_{N_3} & \beta_{12} \\ \beta_{12} & \varepsilon_{CN} \end{pmatrix},$$

where β_{12} represents the coupling between the azide (ε_{N_3}) and nitrile (ε_{CN}) vibrational modes.

From this bilinear coupling model, a shift in the observed absorption peak maxima and a change the relative intensity of the two transitions, which is dependent of the coupling strength, would likely occur when compared to the uncoupled systems. The observed change in relative intensities (10:1 vs. 2.7:1) clearly indicates the presence of coupling.[42] However, due to the large energy difference, 118 cm^{-1}, between the two uncoupled oscillators (2124 cm^{-1} for the azide group[12] and 2241.9 cm^{-1} for the nitrile group[7]), the overall change in energy of the peaks is not expected to be significant. However, it is known that determining

the coupling strength between these two transition dipoles through the splitting in the FTIR spectrum is sometimes difficult.[42]

2D IR spectroscopy is fully capable of measuring vibrational coupling via cross peaks in the off-diagonal region of the spectrum.[49, 56, 57] Therefore, 2D IR was invoked to investigate the coupling for these two vibrational reporters in N_3CNdU. The off-diagonal region (black rectangle – Figure 1) of the spectrum shows the presence of vibrational signatures resulting from coupling between the CN and the N_3 transitions. This coupling appears at T=0 and decreases as a function of waiting times, T, indicative of direct coupling between the dipoles.[56] By fitting the data to a single exponential function the decay of the cross peaks intensity was determined to be 3.5 ± 1.0 ps as a function of the waiting time (see SI). Yet, after 1 ps, the coupling signal is less pronounced, due to the dependence of the signal strength on the average value of the vibrational population decays, T_{10}, and the transition dipole strength. (Figure 2).[52, 57] Since the azide reporter has a shorter lifetime and a larger transition dipole magnitude, the decay of the cross peaks is somewhat dominated by these factors. It should be noted that the overall cross peak intensity is easily measurable despite the weak absorption cross section of the nitrile reporter.[57]

The coupling, β_{12}, is directly measured from the anharmoncity of the off-diagonal peaks, Δ_{12}, from perturbation theory within the weak coupling regime, $|\beta_{12}|/|\varepsilon_{N_3} - \varepsilon_{CN}| < 1$[57]

$$\Delta_{12}=4\Delta\left(\frac{{\beta_{12}}^2}{\left(\varepsilon_{N_3}-\varepsilon_{CN}\right)^2-\Delta^2}\right).$$

A value of 32 ± 1.0 cm^{-1} was calculated for the geometric average of the diagonal anharmonicity, Δ. Using the energy difference between the coupled vibrations (118 cm^{-1}) and the measured off-diagonal anharmonicity of 44 ± 3.3 cm^{-1}, the resulting coupling, β_{12}, is 66.4 ± 5.4 cm^{-1}. The angle was estimated to be 53° ± 1° from the relative intensities of the coupled transitions in the FTIR spectrum (see SI).[37] In an attempt to determine the distance between the reporters transition dipole coupling was implemented, a simple model which assumes coupling is solely due to electrostatic coupling of point dipoles. Using transition dipole coupling (TDC) theory,[58] a distance of 2.9 Å was calculated from the coupling constant and the transition dipole strengths along with the angle between the two dipoles (see SI). It is clear by inspection of the molecule that this distance is an underestimate. However, it is known that transition dipole theory underestimates the coupling strength, because it breaks down at small distances.[42, 50] Thus, a more detailed coupling model is required to obtain a coupling closer to the experimental value.[50]

A more accurate theoretical model to obtain the coupling constant is the finite difference method (FDM). In the FDM method, the coupling constant arises from the derivative of the potential, V, with respect to the local modes, Q_1 and Q_2:

$$\beta_{12}=\frac{\partial^2 V(Q_1,Q_2)}{\partial Q_1 Q_2}.$$

This analytical derivative indicates that the coupling constant has a direct relationship to the curvature of the potential with respect to the local modes.[49, 50] Coupling between two modes can arise from electrostatic, electrodynamics and mechanical contributions within the molecule, sometimes distinguished as through space and through bond contributions. FDM accounts for all of those components whereas TDC only considers through space coupling from electrostatics within a point dipole approximation. Based on the transition dipole densities shown in Figure 5a and 5b, it is suggested that the through bond contributions are minimal. The electrodynamic contributions also do not play a significant role because no transition density is observed when one mode is held at equilibrium and the other mode is displaced.[49]

In order to generate a structural map for this model system, the coupling constants for each dihedral angle were determined by the FDM along the potential energy surface. The structural map relates the coupling constants and the angle between the dipoles to the distance between the two vibrational probes akin to the model put forth by Torii and Tasumi.[48] The dihedral angle is free to rotate in a thermal equilibrium distribution but it is constrained by the steric interactions of the rings and functional groups. At room temperature, several structures are accessible along the PES. Within each minimum, the average coupling constants were calculated to account for this thermal distribution. The average value of the coupling determined for minimum 1 on the PES is approximately 20 cm^{-1} less than the observed experimental coupling. Moreover, the coupling constant at minimum 3 has a value that deviates even more from the experimental findings. Minimum 2, on the other hand, accounts for a coupling constant of 62 cm^{-1} of the dihedral angles within the thermal distribution (0° to 30°). This value is in reasonable agreement with experiment.

To further confirm the position along the PES, the average angle between the dipoles was determined at each minimum. Upon inspection of these angles, minima 1 and 3 are well above the experimental value of 53° ± 1°. The average angle at minimum 2 has a value of 64.3° ± 8.9° which is in close agreement with experiment. Along with the coupling constant, these results indicate that the favorable structural distribution is located within minimum 2 of the PES. Further support of this conformational distribution is shown in previous X-ray crystallographic data on uridine and deoxyuridine[59, 60] as well as the prior theoretical results of these molecules in the gas phase.[61] From the structural map, the distance between the two reporters was determined to be 7.9 ± 0.3 Å. The distances for specific coupling constants and angles between the dipoles range from 5 to 8.5 Å.

Although the calculations suggests that minimum 3 is more thermodynamically favorable than minimum 2 by its slightly lower energy, the experimental values indicate minimum 2 represents the actual thermal distribution. Upon further investigation of the PES using a different water model (Onsager model), it was determined that the minimum at position 3 is higher in energy and less defined (see SI). Both minima 1 and 2 are quite similar for both water models.

In addition to the coupling, significant changes in the spectral shape of both transitions in the diagonal region of the spectrum with waiting time result from homogenization of the frequency distribution. Measurements of the correlation decays for both the azide and nitrile

modes revealed time constants of 1.4 ± 0.1 ps and 1.3 ± 0.2 ps respectively. This observation is expected based on the frequency-frequency correlation decay of typical N_3 and CN modes in water, ~1.5–2 ps.[12, 13] The temporal evolution of the correlation decay manifests itself on the time scales of motions associated with the surrounding solvent molecules. The observed time constants match the characteristic timescale, 0.8–2 ps, for the making and breaking of hydrogen bonds between water molecules and polar solutes.[62–68] Using azide and nitrile groups, 2D IR spectra of these probes captures the dephasing[69] times at two distinct locations within the same molecule. In this case, the two reporters are simultaneously measuring the same local water dynamics. However, it is likely that the vibrational dynamics will vary in larger biological systems when these two reporters are on separate nucleosides and in different local environments.

In principle, this pair of reporters can effectively detect the local vibrational dynamics around each reporter and correlate it to the larger structural motions measured by vibrational coupling. By placing these probes on separate nucleotides, this utility can be extended to detect even larger distances in these types of systems. This multi-faceted source of spectral informational provided by the azide and nitrile groups within a single molecule afford a set vibrational reporters capable of investigating the structural diversity found in RNA apartmers. Furthermore, this dual nature of detection combined with the spectrally isolated frequencies of vibration and reasonable oscillator strengths will prove useful in detecting the mobility of water as well as local field fluctuations that may result from small hinging motions in larger RNA structures, akin to the sidechain motions[36] detected in peptides.

Conclusions

The symmetric stretch of the CN mode and the asymmetric stretch of the N_3 mode have been examined in tandem by two-dimensional infrared spectroscopy in water. By inclusion of both vibrational reporters in the same biomolecule, both the correlation decay (~1.4 ps) and the vibrational coupling (~66 cm^{-1}) between the two transitions can easily be measured. The distance determined from TDC (2.9 Å) is unreasonable considering the chemical structure suggesting that TDC is insufficient for certain cases. By the use of the finite difference method, a theoretical model was generated that maps the distance between the probes to the coupling constant and the angle between the dipoles. Upon application of this model, the average distance between the two reporters was measured to be approximately 7.9 Å. With an accurate coupling model, a ‘spectroscopic ruler’ within the range of 5–8.5 Å has been established. Furthermore, the correlation decay measured for each probe affirms that the mobility of water can be detected at two different locations within the molecule. Thus, the combination of this pair of reporters provides a spectroscopic tool for monitoring structural changes and correlating these changes to the dynamics of water within nucleic acid systems.

Supplementary Material

Refer to Web version on PubMed Central for supplementary material.

Acknowledgments

This work was supported in part by NIH (R15GM093330) to SHB/EEF.

REFERENCES

1. Getahun Z, Huang CY, Wang T, De Leon B, DeGrado WF, Gai F. Using nitrile-derivatized amino acids as infrared probes of local environment. J. Am. Chem. Soc. 2003; 125:405–411. [PubMed: 12517152]
2. Oh KI, Lee JH, Joo C, Han H, Cho M. beta-Azidoalanine as an IR probe: Application to amyloid A beta(16–22) aggregation. J. Phys. Chem. B. 2008; 112:10352–10357. [PubMed: 18671422]
3. Silverman LN, Pitzer ME, Ankomah PO, Boxer SG, Fenlon EE. Vibrational stark effect probes for nucleic acids. J. Phys. Chem. B. 2007; 111:11611–11613. [PubMed: 17877390]
4. Suydam IT, Boxer SG. Vibrational Stark effects calibrate the sensitivity of vibrational probes for electric fields in proteins. Biochemistry. 2003; 42:12050–12055. [PubMed: 14556636]
5. Tucker MJ, Getahun Z, Nanda V, DeGrado WF, Gai F. A new method for determining the local environment and orientation of individual side chains of membrane-binding peptides. J. Am. Chem. Soc. 2004; 126:5078–5079. [PubMed: 15099085]
6. Tucker MJ, Kim YS, Hochstrasser RM. 2D IR photon echo study of the anharmonic coupling in the OCN region of phenyl cyanate. Chem. Phys. Lett. 2009; 470:80–84. [PubMed: 20160952]
7. Watson MD, Gai XS, Gillies AT, Brewer SH, Fenlon EE. A Vibrational Probe for Local Nucleic Acid Environments: 5-Cyano-2 '-deoxyuridine. J. Phys. Chem. B. 2008; 112:13188–13192. [PubMed: 18816094]
8. Ye SX, Huber T, Vogel R, Sakmar TP. FTIR analysis of GPCR activation using azido probes. Nat. Chem. Biol. 2009; 5:397–399. [PubMed: 19396177]
9. Jo H, Culik RM, Korendovych IV, DeGrado WF, Gai F. Selective Incorporation of Nitrile-Based Infrared Probes into Proteins via Cysteine Alkylation. Biochemistry. 2010; 49:10354–10356. [PubMed: 21077670]
10. Gai XS, Coutifaris BA, Brewer SH, Fenlon EE. A direct comparison of azide and nitrile vibrational probes. Phys. Chem. Chem. Phys. 2011; 13:5926–5930. [PubMed: 21336362]
11. Fang C, Bauman JD, Das K, Remorino A, Arnold E, Hochstrasser RM. Two-dimensional infrared spectra reveal relaxation of the nonnucleoside inhibitor TMC278 complexed with HIV-1 reverse transcriptase. Proc. Natl. Acad. Sci. U. S. A. 2008; 105:1472–1477. [PubMed: 18040050]
12. Tucker MJ, Gai XS, Fenlon EE, Brewer SH, Hochstrasser RM. 2D IR photon echo of azido-probes for biomolecular dynamics. Phys. Chem. Chem. Phys. 2010; 13:2237–2241. [PubMed: 21116553]
13. Urbanek DC, Vorobyev DY, Serrano AL, Gai F, Hochstrasser RM. The Two-Dimensional Vibrational Echo of a Nitrile Probe of the Villin HP35 Protein. Journal of Physical Chemistry Letters. 2010; 1:3311–3315. [PubMed: 21132120]
14. Liu H, Lantz R, Cosme P, Rivera N, Andino C, Gonzalez WG, Terentis AC, Wojcikiewicz EP, Oyola R, Miksovska J, Du D. Site-specific dynamics of amyloid formation and fibrillar configuration of A beta(1–23) using an unnatural amino acid. Chem. Commun. 2015; 51:7000–7003.
15. Zhang W, Markiewicz BN, Doerksen RS, Smith AB III, Gai F. C≡N stretching vibration of 5-cyanotryptophan as an infrared probe of protein local environment: what determines its frequency? Phys. Chem. Chem. Phys. 2015; 18:7027–7034.
16. Bagchi S, Boxer SG, Fayer MD. Ribonuclease S Dynamics Measured Using a Nitrile Label with 2D IR Vibrational Echo Spectroscopy. J. Phys. Chem. B. 2012; 116:4034–4042. [PubMed: 22417088]
17. Chung JK, Thielges MC, Fayer MD. Dynamics of the folded and unfolded villin headpiece (HP35) measured with ultrafast 2D IR vibrational echo spectroscopy. Proc. Natl. Acad. Sci. U. S. A. 2011; 108:3578–3583. [PubMed: 21321226]
18. Suydam IT, Snow CD, Pande VS, Boxer SG. Electric fields at the active site of an enzyme: Direct comparison of experiment with theory. Science. 2006; 313:200–204. [PubMed: 16840693]

19. Maienschein-Cline MG, Londergan CH. The CN stretching band of aliphatic thiocyanate is sensitive to solvent dynamics and specific solvation. J. Phys. Chem. A. 2007; 111:10020–10025. [PubMed: 17867661]
20. Le Sueur AL, Horness RE, Thielges MC. Applications of two-dimensional infrared spectroscopy. Analyst. 2015; 140:4336–4349. [PubMed: 26007625]
21. Waegele MM, Culik RM, Gai F. Site-Specific Spectroscopic Reporters of the Local Electric Field, Hydration, Structure, and Dynamics of Biomolecules. J. Phys. Chem. Lett. 2011; 2:2598–2609. [PubMed: 22003429]
22. Ma JQ, Pazos IM, Zhang WK, Culik RM, Gai F. Site-Specific Infrared Probes of Proteins. Annu. Rev. Phys. Chem. 2015; 66:357–377. [PubMed: 25580624]
23. Park KH, Jeon J, Park Y, Lee S, Kwon HJ, Joo C, Park S, Han H, Cho M. Infrared Probes Based on Nitrile-Derivatized Prolines: Thermal Insulation Effect and Enhanced Dynamic Range. J. Phys. Chem. Lett. 2013; 4:2105–2110.
24. Kim H, Cho M. Infrared Probes for Studying the Structure and Dynamics of Biomolecules. Chem. Rev. 2013; 113:5817–5847. [PubMed: 23679868]
25. Bazewicz CG, Liskov MT, Hines KJ, Brewer SH. Sensitive, Site-Specific, and Stable Vibrational Probe of Local Protein Environments: 4-Azidomethyl-L-Phenylalanine. J. Phys. Chem. B. 2013; 117:8987–8993. [PubMed: 23865850]
26. Nagarajan S, Taskent-Sezgin H, Parul D, Carrico I, Raleigh DP, Dyer RB. Differential Ordering of the Protein Backbone and Side Chains during Protein Folding Revealed by Site-Specific Recombinant Infrared Probes. J. Am. Chem. Soc. 2011; 133:20335–20340. [PubMed: 22039909]
27. Taskent-Sezgin H, Chung JA, Banerjee PS, Nagarajan S, Dyer RB, Carrico I, Raleigh DP. Azidohomoalanine: A Conformationally Sensitive IR Probe of Protein Folding, Protein Structure, and Electrostatics. Angew. Chem.-Int. Edit. 2010; 49:7473–7475.
28. Gai XS, Fenlon EE, Brewer SH. A Sensitive Multispectroscopic Probe for Nucleic Acids. J. Phys. Chem. B. 2010; 114:7958–7966. [PubMed: 20496915]
29. Gillies AT, Gai XS, Buckwalter BL, Fenlon EE, Brewer SH. N-15 NMR Studies of a Nitrile-Modified Nucleoside. J. Phys. Chem. B. 2010; 114:17136–17141. [PubMed: 21126044]
30. Kim YS, Hochstrasser RM. Chemical exchange 2D IR of hydrogen-bond making and breaking. Proc. Natl. Acad. Sci. U. S. A. 2005; 102:11185–11190. [PubMed: 16040800]
31. Zheng JR, Kwak K, Asbury J, Chen X, Piletic IR, Fayer MD. Ultrafast dynamics of solute-solvent complexation observed at thermal equilibrium in real time. Science. 2005; 309:1338–1343. [PubMed: 16081697]
32. Edler J, Hamm P. Two-dimensional vibrational spectroscopy of the amide I band of crystalline acetanilide: Fermi resonance, conformational substates, or vibrational self-trapping? J. Chem. Phys. 2003; 119:2709–2715.
33. Fang C, Wang J, Charnley AK, Barber-Armstrong W, Smith AB, Decatur SM, Hochstrasser RM. Two-dimensional infrared measurements of the coupling between amide modes of an alpha-helix. Chem. Phys. Lett. 2003; 382:586–592.
34. Fang C, Wang J, Kim YS, Charnley AK, Barber-Armstrong W, Smith AB, Decatur SM, Hochstrasser RM. Two-dimensional infrared spectroscopy of isotopomers of an alanine rich alpha-helix. J. Phys. Chem. B. 2004; 108:10415–10427.
35. Kumar K, Sinks LE, Wang JP, Kim YS, Hochstrasser RM. Coupling between C-D and C=O motions using dual-frequency 2D IR photon echo spectroscopy. Chem. Phys. Lett. 2006; 432:122–127.
36. Bagchi S, Charnley AK, Smith AB III, Hochstrasser RM. Equilibrium Exchange Processes of the Aqueous Tryptophan Dipeptide. J. Phys. Chem. B. 2009; 113:8412–8417. [PubMed: 19459617]
37. Remorino A, Hochstrasser RM. Three-Dimensional Structures by Two-Dimensional Vibrational Spectroscopy. Accounts Chem. Res. 2012; 45:1896–1905.
38. Stryer L. Fluorescence energy-transfer as a spectroscopic ruler. Annu. Rev. Biochem. 1978; 47:819–846. [PubMed: 354506]
39. Rabenstein MD, Shin YK. Determination of the distance between 2 spin labels attached to a macromolecular. Proc. Natl. Acad. Sci. U. S. A. 1995; 92:8239–8243. [PubMed: 7667275]

40. Chen H, Wen X, Li J, Zheng J. Molecular Distances Determined with Resonant Vibrational Energy Transfers. J. Phys. Chem. A. 2014; 118:2463–2469. [PubMed: 24641170]
41. Li J, Bian H, Chen H, Wen X, Hoang BT, Zheng J. Ion Association in Aqueous Solutions Probed through Vibrational Energy Transfers among Cation, Anion, and Water Molecules. J. Phys. Chem. B. 2013; 117:4274–4283. [PubMed: 22928938]
42. Krummel AT, Zanni MT. Evidence for coupling between nitrile groups using DNA templates: A promising new method for monitoring structures with infrared spectroscopy. J. Phys. Chem. B. 2008; 112:1336–1338. [PubMed: 18197662]
43. Polushin NN, Smirnov IP, Verentchikov AN, Coull JM. Synthesis of oligonucleotides containing 2'-azido- and 2'-amino-2'-deoxyuridine using phosphotriester chemistry. Tetrahedron Lett. 1996; 37:3227–3230.
44. Jawalekar AM, Meeuwenoord N, Cremers JGO, Overkleeft HS, van der Marel GA, Rutjes F, van Delft FL. Conjugation of nucleosides and oligonucleotides by [3+2] cycloaddition. J. Org. Chem. 2008; 73:287–290. [PubMed: 18052191]
45. Sylvers LA, Wower J. Nucleic acid-incorporated azidonucleotides - probes for studying the interaction of RNA OR DNA with proteins and other nucleic-acids. Bioconjugate Chem. 1993; 4:411–418.
46. Aigner M, Hartl M, Fausterm K, Steger J, Bister K, Micura R. Chemical Synthesis of Site-Specifically 2'-Azido-Modified RNA and Potential Applications for Bioconjugation and RNA Interference. ChemBioChem. 2011; 12:47–51. [PubMed: 21171007]
47. Kim YS, Wang J, Hochstrasser RM. Two-dimensional infrared spectroscopy of the alanine dipeptide in aqueous solution. J. Phys. Chem. B. 2005; 109:7511–7521. [PubMed: 16851862]
48. Torii H, Tasumi M. Ab initio molecular orbital study of the amide I vibrational interactions between the peptide groups in di- and tripeptides and considerations on the conformation of the extended helix. J. Raman Spectrosc. 1998; 29:81–86.
49. Krummel AT, Zanni MT. DNA vibrational coupling revealed with two-dimensional infrared spectroscopy: Insight into why vibrational spectroscopy is sensitive to DNA structure. J. Phys. Chem. B. 2006; 110:13991–14000. [PubMed: 16836352]
50. Moran A, Mukamel S. The origin of vibrational mode couplings in various secondary structural motifs of polypeptides. Proc. Nat. Acad. Sci. USA. 2004; 101:506–510. [PubMed: 14704267]
51. Lipkin JS, Song R, Fenlon EE, Brewer SH. Modulating Accidental Fermi Resonance: What a Difference a Neutron Makes. J. Phys. Chem. Lett. 2011; 2:1672–1676.
52. Hamm P, Hochstrasser RM. Structure and dynamics of proteins and peptides: femtosecond two-dimensional infrared spectroscopy. Pract. Spectrosc. 2001; 26:273–347.
53. Kwac K, Cho MH. Molecular dynamics simulation study of N-methylacetamide in water. II. Two-dimensional infrared pump-probe spectra. J. Chem. Phys. 2003; 119:2256–2263.
54. Kwak K, Park S, Finkelstein IJ, Fayer MD. Frequency-frequency correlation functions and apodization in two-dimensional infrared vibrational echo spectroscopy: A new approach. J. Chem. Phys. 2007; 127
55. Kwak K, Rosenfeld DE, Fayer MD. Taking apart the two-dimensional infrared vibrational echo spectra: More information and elimination of distortions. J. Chem. Phys. 2008; 128
56. DeFlores LP, Ganim Z, Ackley SF, Chung HS, Tokmakoff A. The anharmonic vibrational potential and relaxation pathways of the amide I and II modes of N-methylacetamide. J. Phys. Chem. B. 2006; 110:18973–18980. [PubMed: 16986892]
57. Hamm P, Lim M, DeGrado WF, Hochstrasser RM. The two-dimensional IR nonlinear spectroscopy of a cyclic penta-peptide in relation to its three-dimensional structure. Proc. Nat. Acad. Sci. USA. 1999; 96:2036–2041. [PubMed: 10051590]
58. Torii H, Tasumi M. Model-Calculations on the Amide-I Infrared Bands of Globular-Proteins. J. Chem. Phys. 1992; 96:3379–3387.
59. Green EA, Rosenstein RD, Shiono R, Abraham DJ. The Crystal Structure of Uridine. Acta Crystallogr. B. 1975; B31:102–107.
60. Rahman A, Wilson HR. The Crystal and Molecular Structure of Deoxyuridine. Acta Crystallogr. B. 1972; B28:2260–2270.

61. Delchev VB. Computational (DFT and TD DFT) study of the electron structure of the tautomers/conformers of uridine and deoxyuridine and the processes of intramolecular proton transfers. J. Mol. Model. 2010; 16:749–757. [PubMed: 19820971]
62. Kuroda DG, Vorobyev DY, Hochstrasser RM. Ultrafast relaxation and 2D IR of the aqueous trifluorocarboxylate ion. J. Chem. Phys. 2010; 132
63. Bakker HJ, Skinner JL. Vibrational Spectroscopy as a Probe of Structure and Dynamics in Liquid Water. Chem. Rev. 2010; 110:1498–1517. [PubMed: 19916491]
64. Kumar R, Schmidt JR, Skinner JL. Hydrogen bonding definitions and dynamics in liquid water. J. Chem. Phys. 2007; 126
65. Hamm P, Lim MH, Hochstrasser RM. Structure of the amide I band of peptides measured by femtosecond nonlinear-infrared spectroscopy. J. Phys. Chem. B. 1998; 102:6123–6138.
66. Schmidt JR, Corcelli SA, Skinner JL. Ultrafast vibrational spectroscopy of water and aqueous N-methylacetamide: Comparison of different electronic structure/molecular dynamics approaches. J. Chem. Phys. 2004; 121:8887–8896. [PubMed: 15527353]
67. DeCamp MF, DeFlores L, McCracken JM, Tokmakoff A, Kwac K, Cho M. Amide I vibrational dynamics of N-methylacetamide in polar solvents: The role of electrostatic interactions. J. Phys. Chem. B. 2005; 109:11016–11026. [PubMed: 16852342]
68. Kim YS, Liu L, Axelsen PH, Hochstrasser RM. 2D IR provides evidence for mobile water molecules in beta-amyloid fibrils. Proc. Nat. Acad. Sci. USA. 2009; 106:17751–17756. [PubMed: 19815514]
69. Hamm P, Lim M, Hochstrasser RM. Non-Markovian dynamics of the vibrations of ions in water from femtosecond infrared three-pulse photon echoes. Phys. Rev. Lett. 1998; 81:5326–5329.

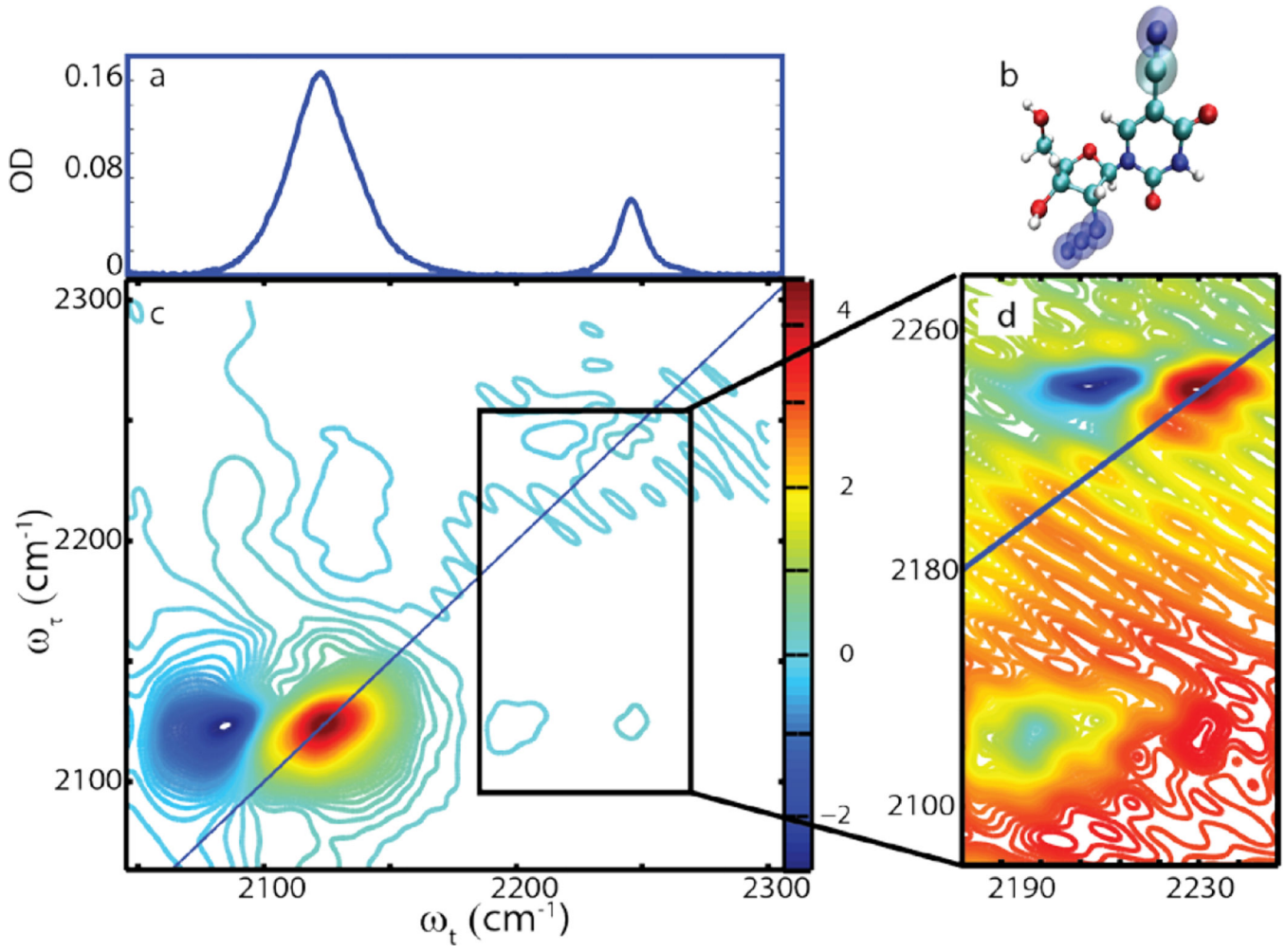

Figure 1.

(a) Linear IR, (c) absorptive 2D IR spectra and (d) expanded cross peak region and diagonal peaks of the CN transition observed in the 2D IR spectra of N_3CNdU in water at waiting T = 200 fs. (b) Structure of 2'-azido-5-cyano-2'-deoxyuridine highlighting the nitrile and azide reporters.

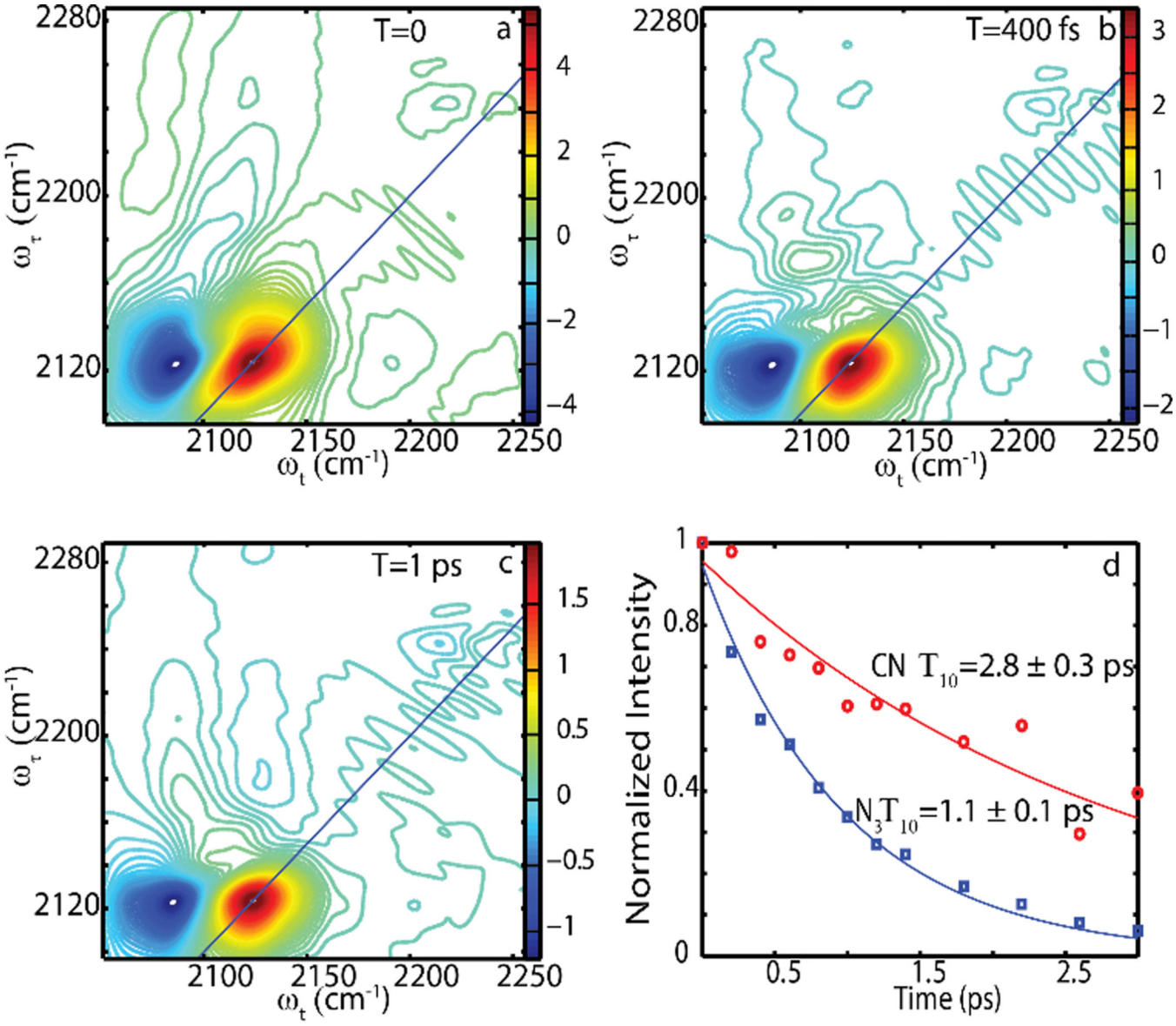

Figure 2.

2D IR spectra of N_3CNdU in water at waiting time: a) T = 0, b) T = 400 fs, c) T = 1.0 ps. d) Vibrational lifetime decays of N_3 and CN transitions in N_3CNdU.

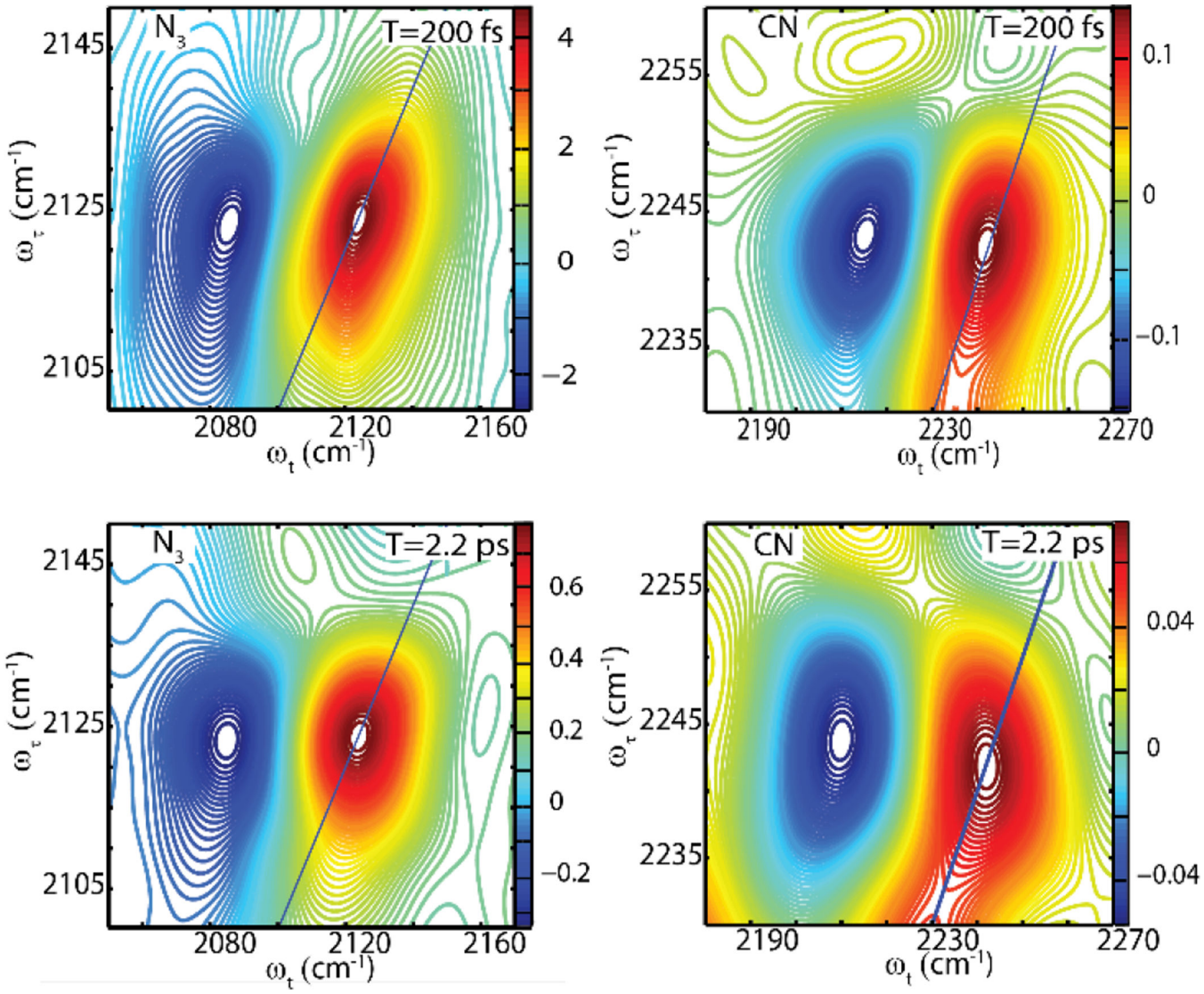

Figure 3.

Real part of the absorptive 2D IR spectra of N_3CNdU in water for (left) N_3 and (right) CN at waiting times T=200 fs and T=2.2 ps.

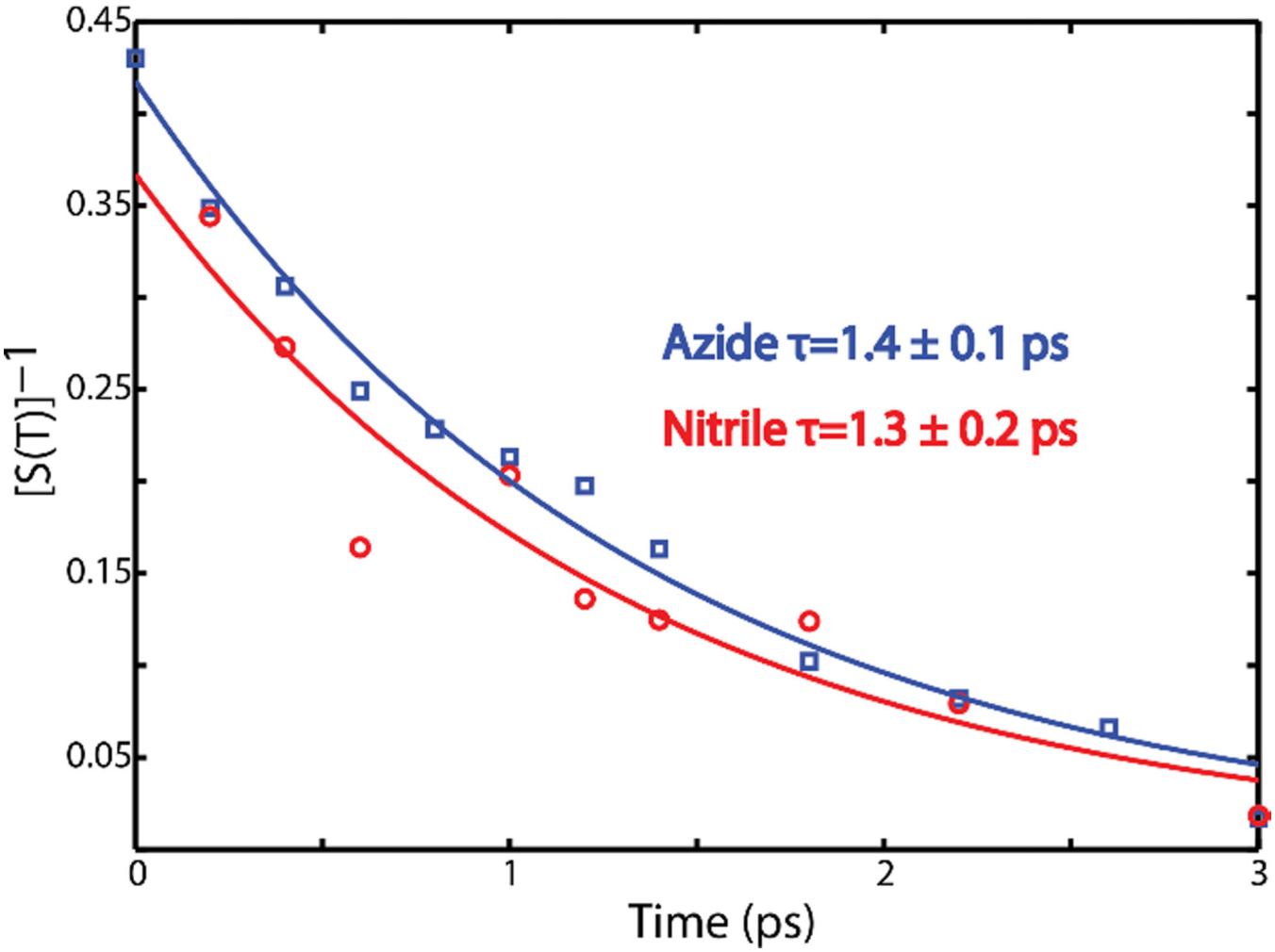

Figure 4.
Inverse slope $[S(T)]^{-1}$ vs waiting time of (red) CN symmetric stretch and (blue) N_3 asymmetric stretch in water.

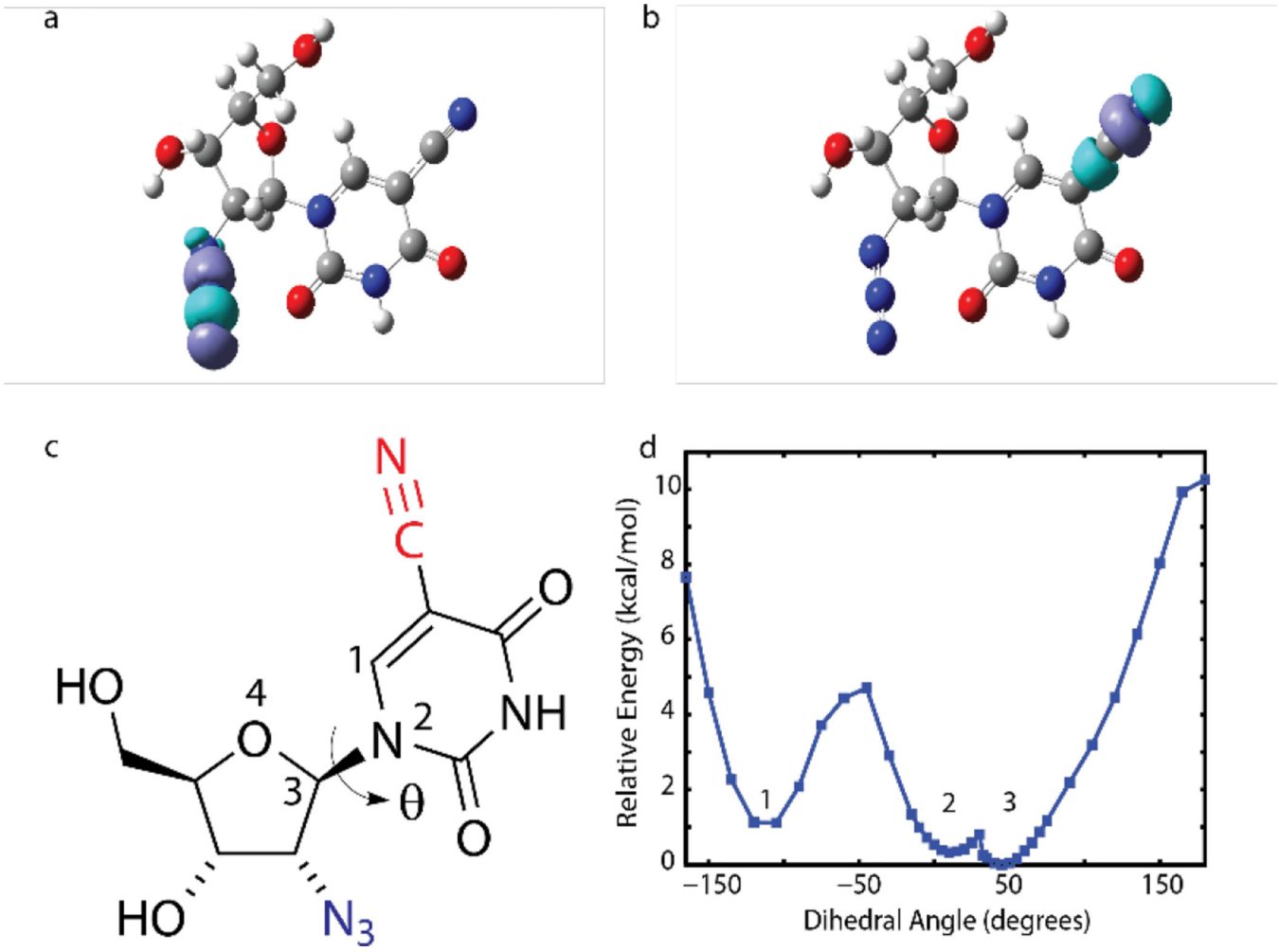

Figure 5.

Transition densities of (a) N_3 and (b) CN. (c) N_3CNdU molecule with the labeled atoms that represent the dihedral angle of interest and (d) the calculated relative energies at different dihedral angles.